Available online at www.sciencedirect.com
ScienceDirect
Colloids and Surfaces A: Physicochem. Eng. Aspects 323 (2008) 19–27
COLLOIDS AND SURFACES A
www.elsevier.com/locate/colsurfa

Motion of viscous drops on superhydrophobic surfaces due to magnetic gradients

John Schneider [a], Ana Egatz-Gómez [a], Sonia Melle [a,b,*], S. Lindsay [a], P. Domínguez-García [c], M.A. Rubio [c], M. Márquez [a], Antonio A. García [a,**]

[a] *Harrington Department of Bioengineering, Arizona State University (ASU), Tempe, AZ 85287, United States*
[b] *Departamento de Óptica, UCM, Arcos de Jalón s/n, 28037 Madrid, Spain*
[c] *Departamento de Física Fundamental, UNED, Senda del Rey 9, 28040 Madrid, Spain*

Received 30 May 2007; received in revised form 11 September 2007; accepted 4 October 2007
Available online 13 October 2007

Abstract

Microliter droplets that contain paramagnetic particles can be moved on superhydrophobic surfaces using magnetic fields. Paramagnetic microparticles form chains at concentrations ranging from 0.1 to 10 wt% and are used to move, coalesce, and split drops of water as well as drops of biological fluids. Video analysis of dextran solution drops to investigate the effect of viscosity on drop movement on LPDE surfaces suggests that paramagnetic particle chain orientation compensates for viscosity increases from 1.2 mPa s (water) to 125 mPa s (20%, w/v – Dextran 428) in order to maintain drop movement. Interestingly, such changes in chain orientation are not present for drops moving on silicon nanowire (Si NW) superhydrophobic surfaces even at higher viscosities 470 mPa s (30% w/v – Dextran 428). On Si NW surfaces, drops with high viscosity can be moved even with particle concentrations as low as 0.5%. Higher particle concentrations (2%) are needed to displace drops on LPDE surfaces. This new approach to so-called "discrete" microliter-scale fluidics has the advantages of faster and more flexible control over drop movement, manipulation, and detection of solution components.

Keywords: Superhydrophobic surface; Paramagnetic particle; Microfluidics; Drops; Silicon nanowire surface; Low-density polyethylene surface

1. Introduction

The past decade and a half has given rise to much research and development of devices that can move very small amounts of liquids. Terms such as microfluidics and even nanofluidics have been used to describe this activity. Parallel to this effort has been a large body of work on creating superhydrophobic surfaces. For the most part, these two fields of study and development have remained nearly separate. In order to lay the foundation to help explain why combining these two fields can lead to some useful new capabilities, it is instructive to introduce key ideas in these fields before describing our work in discrete micro-scale fluidics using magnetic control.

The physics of scale requires that micro-scale fluidic devices exploit new approaches to fluid movement since they have an inherently large ratio of liquid surface area to volume. Along these lines, interest in mimicking the water repellent properties of lotus leaves has led to reports of superhydrophobic surfaces that combine hydrophobic molecular coatings with surface roughness characterized by either well-ordered microstructures [1,2] or random fractal geometry [3]. Rough fractal surfaces are particularly interesting due to the extremely high degree of roughness they possess. Wenzel proposed that the effect of roughness is to enhance the inherent wetting behavior of the surface (by increasing the contact angle >90°, or by decreasing the contact angle <90°) [4]. However, for randomly rough or

* Corresponding author at: Harrington Department of Bioengineering, Arizona State University (ASU), Tempe, AZ 85287, United States.
** Corresponding author at: Department of Optics, Complutense University of Madrid, Madrid 28037, Spain.
E-mail addresses: smelle@fis.ucm.es (S. Melle), tony.garcia@asu.edu (A.A. García).

0927-7757/$ – see front matter © 2007 Elsevier B.V. All rights reserved.
doi:10.1016/j.colsurfa.2007.10.011

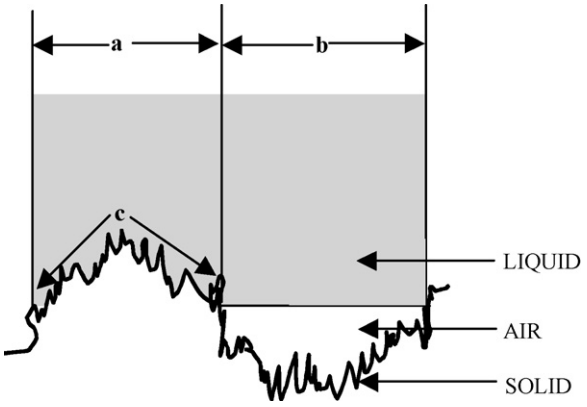

Fig. 1. Drop of liquid sitting on a randomly rough composite surface made up of solid and air.

fractal surfaces and if the fractal behavior extends to the molecular scale, fluids having different molecular dimensions would experience different solid–fluid interfacial areas. A thermodynamic model for the equilibrium contact angle which takes into account both the fractal nature of the surface and the relative dimensions of the different fluid molecules has been developed [5]. Depending on the relative sizes of the fluid molecules and their wetting tendencies, the contact angle on randomly rough or fractal surfaces can either be higher or lower than the contact angle for a smooth surface. Fig. 1 shows a drop of liquid sitting on a fractally rough composite surface made up of solid and air.

In the case of rough porous surfaces, the Cassie–Baxter equation describes the equilibrium contact angle on a composite surface that retains pockets of air underneath the sessile drop [6]. This equation uses the ratio of projected areas of the solid surface–liquid and air surface–liquid interfaces, respectively, to the total projected area in order to predict the contact angle on a rough surface using smooth surface contact angle data. While it is possible to calculate these rations for well-defined Euclidian surfaces, fractal surfaces are not amenable to this quantitative treatment. Therefore, for all practical purposes this may have to be an adjustable parameter.

Both Wenzel and Cassie–Baxter equations represent local energy minima in drop conformation, and it can be shown that for randomly rough surfaces the Wenzel contact angle is always less than or equal to the Cassie contact angle. Patankar [7] has found that the equilibrium drop shape with the lower value of apparent contact angle on rough, well-ordered surfaces will have lower energy. If this result can be extended to randomly rough surfaces, the Wenzel contact angle will always represent the global energy minimum of the system. At intrinsic contact angles of >90°, the apparent contact angles (Wenzel and Cassie–Baxter) increase as a function of the roughness of the surface, as represented by the fractal dimension, till the physical limit of an apparent 180° contact angle is reached.

We have found that reaching the limit of 180° contact angle (e.g. the so-called “Lotus-Effect”) is important to reduce the friction for an aqueous solution drop moving on a surface in order to control drop movement using an external field. The “Lotus-Effect” can be best illustrated by the sequence of frames from a digital movie shown in Fig. 2. In this example, half of the slide contains a very rough surface comprising nanowires and the entire slide is coated with a fluorinated hydrocarbon. In Fig. 2(a) and (b), the water drops are placed on the side of the silicon substrate that is flat and covalently coated with a fluoronated hydrocarbon. In Fig. 2(c), the water drops have slid off the side of the substrate containing nanowires and a covalent coating of fluorinated hydrocarbon.

Rather than simply having drops slide off the superhydrophobic surface, micro-scale fluidics requires a method to exert control over the direction and speed at which a droplet moves. Droplet motion and control in discrete micro-scale fluidics using magnetism is the interplay between attractive forces among paramagnetic particles in the presence of an external magnetic field and a superhydrophobic surface.

In order to place a water droplet on a superhydrophobic surface without it falling off, paramagnetic particles are added to the drop and a magnetic field is applied at the location of drop placement. One requirement for this method is that the superhydrophobic surface should have advancing and receding contact angles near 180° so that the frictional resistance to movement is very low.

Recently, we have found that in order to move the drop we must move the magnetic field. Due to the low-frictional resistance the drop can be moved at speeds up to 7 cm/s [8], in three dimensions [9], and other interesting additional effects such as drop splitting and coalescence [10] can be observed. Biological fluids can have substantially higher viscosities than water. Blood can have complex rheological behavior and is nearly four times as viscous as water depending upon temperature, flow rate, and red blood cell count. Plasma is about 1.8 times more viscous than water, depending upon protein concentration. At low-shear rates, human saliva can be up to five times more viscous than water

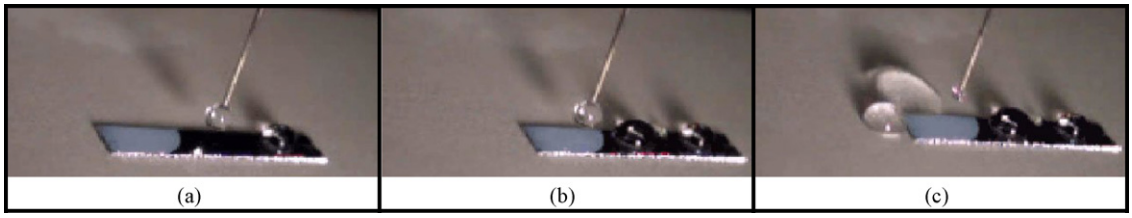

Fig. 2. Three frames from a movie showing the difference between a hydrophobic and a superhydrophobic surface. The left-hand side of this silicon substrate contains nanowires while the right hand side does not (a–c). The entire surface is covalently coated with a fluorinated hydrocarbon. The water drops from the needle adhere to the right-hand side of the sample (a and b) while they slide off the left-hand side of the sample (c).

[11]. We are interested in applying discrete magnetofluidics for diagnostic purposes and for that reason, studying how fluid viscosity affects drop movement is an essential issue. In addition, the sliding motion of the drops deserves some comment. Fluid drops surrounded by another fluid can show multiple types of motion depending on drop shape, size, and viscosity contrast. For instance, slipping, sliding, rolling, and tank-treading motions have been described in the case of drops slowly moving under a gravity body force on inclined plates. In such a case, the shape of the drop is controlled by the Bond number, $B_0 = \Delta\rho g R^2/\gamma$, where $\Delta\rho$ is the density difference between both fluids, g the acceleration due to gravity, R the drop radius, and γ is the liquid–air surface tension. Low-B_0 values correspond to drops with a nearly spherical shape, medium-B_0 values correspond to drops with a flattened contact plate (flat spot drops), and high-B_0 values correspond to pancake shaped drops. It is known that flat spot and pancake drops with higher viscosity than the surrounding fluid should perform a sliding motion [12]. In the experiments reported here, we are dealing with flat spot water drops in air with a high-viscosity contrast. Therefore, sliding motion should be expected. In this paper, we present an analysis of drop motion that includes a combination of surface and fluid properties.

2. Experimental materials and methods

2.1. Silicon nanowire surfaces

In order to create a superhydrophobic nanowire surface, we use vapor–liquid–solid (VLS) growth systems to create high-aspect ratio Si nanowires with various diameters, spacing, and lengths. These Si nanostructures are easily fabricated for subsequent air oxidation and functionalization with molecular coatings. Self-assembled nanodots, formed during evaporation of a few monolayers of Au, are used as metal catalytic seeds to grow one-dimensional nanowires on the surface and create a particular surface morphology [9]. During subsequent VLS synthesis, the Au dots form a eutectic liquid with Si from which liquid-mediated growth of single crystal Si nanowires occurs. The nanowire diameters are set by the Au dot diameters, with one-dimensional growth occurring as the AuSi eutectic dot rides along at the free end of the growing wire. The length of the nanowires is easily controlled by fixing the growth time (Fig. 3). The Au dots at the end of the nanowires account for only a very small area and can be chemically removed to eliminate any effect they may have on interfacial properties. Finally, the Si nanowire substrates were covalently coated with a perfluorinated hydrocarbon in order to obtain superhydrophobic samples.

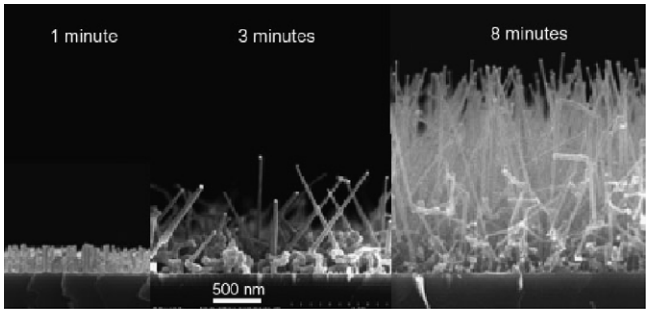

Fig. 3. SEM image sequence illustrating how the nanowire length and topology can be tailored by varying the growth time from 1 to 8 min.

2.2. Low-density polyethylene surfaces

Superhydrophobic low-density polyethylene (LDPE) surfaces were prepared by adapting the method of Lu et al. [13]. Briefly, LDPE was chosen as the substrate for its inherent hydrophobicity, low cost, and flexibility. LDPE pellets were dissolved in xylene. After the LDPE had fully dissolved, MEK (a nonsolvent for LDPE) was added to the solvent-plastic solution to increase surface roughness and aqueous drop contact angle [14]. The solution temperature and solvent evaporation were controlled for tailored crystallization [9].

2.3. Paramagnetic particles

We used carbonyl iron particles (Sigma–Aldrich Inc., St Louis, MO) with sizes ranging from 6 to 9 μm, and high-magnetic saturation. These particles are usually regarded as paramagnetic or superparamagnetic, because their magnetization curve (M–H curve) has a small or null hysteresis, little or no magnetic remanence, and their magnetic response is linear for applied magnetic fields of small intensity [15]. For this study, carbonyl iron microparticles were coated with polysiloxane following the procedure to prevent oxidation [16]. The polysiloxane coating only slightly affected the magnetic properties of the particles, reducing the magnetic saturation value of the carbonyl iron microparticles from approximately 225 to 191 emu/g and increasing the coercive field from approximately 1.3 Oe for the uncoated microparticles to 6.5 Oe for the polysiloxane-coated microparticles.

2.4. Drop solution

A series of experiments using aqueous solutions of Dextran 428 (i.e., molecular weight of 428,000 Da) were conducted in order to determine whether operating conditions needed to be altered in order to move viscous drops. For a given superhydrophobic surface and keeping drop size (10 μl) and magnetic field strength constant, digital videos were obtained for the movement of drops at 0, 5, 10, and 20% (w/v) Dextran 428 in water, with magnetic microparticle concentrations of 0.5, 2 and 4% (w/v). Dextran dramatically increases the solution viscosity while keeping the aqueous surface tension relatively constant

Table 1
Disc rheometer viscosity measurements for Dextran 428 water solutions at 20 °C

Dextran 428 in water (%, w/v)	Viscosity (mPa s)
0	1.2
5	17
10	28
20	125

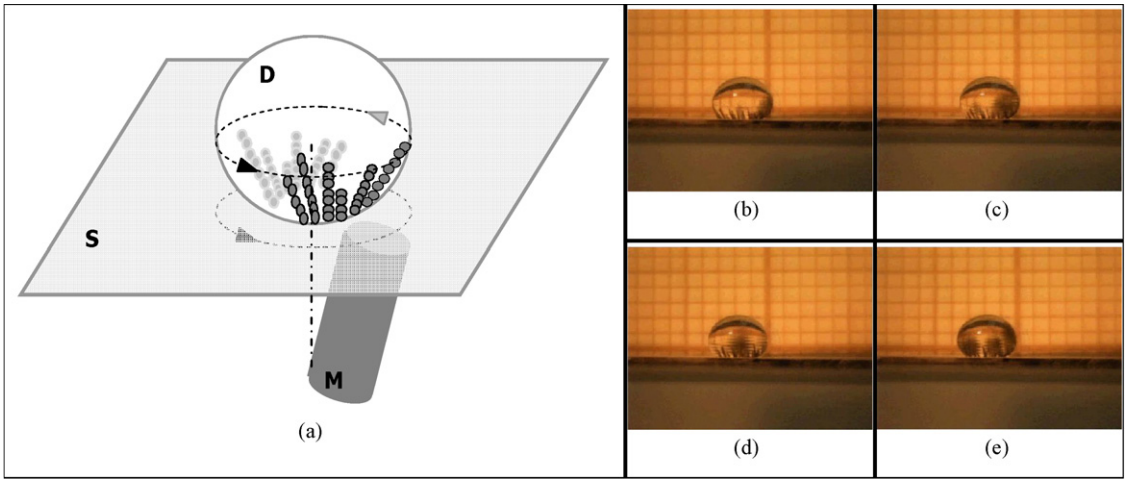

Fig. 4. Schematic diagram (a) and sequence of frames from a video (d–e) showing a drop rotating due to the action of spinning the magnetic field. M, magnet; S, superhydrophobic surface; D, drop. The aligned particle clusters are seen to rotate counter clockwise with perspective looking down at the drop from above.

since it is not surface active [17]. Measurements of viscosity using a disc rheometer are given in Table 1. The measured values agree with predictions of viscosity using the model of Rotureau et al. [18], and Dextran 500 viscosity data from a manufacturer [19].

3. Results and discussion

We briefly describe and summarize the capabilities of aqueous drop movement and control using superhydrophobic surfaces, paramagnetic particles and magnetic fields. Small water drops (volume 5–15 μl) that contain fractions of paramagnetic particles as low as 0.1% in weight can be moved on a superhydrophobic surface at relatively high speed (7 cm/s) by displacing a permanent magnet. Within this volume range, drops are not visibly affected by gravity and remain nearly spherical when placed on superhydrophobic surfaces. The magnetic force required to initiate drop movement is not affected by the drop size and increases upon decreasing the particle concentration. Coalescence of two drops has been demonstrated by moving a drop that contains paramagnetic particles towards an aqueous drop that was previously pinned to a surface defect making it possible to move the newly combined drop with the magnetic field. A drop can also be split using two permanent magnets [8]. Coating the magnetic microparticles with polysiloxane in order to prevent oxidation does not visibly affect the magnetically controlled drop movement [10]. Other superhydrophobic surfaces such as those obtained by LDPE crystallisation have been also studied. Plastic superhydrophobic surfaces can be made in 3D shapes and can be made more economically thus making them potentially very attractive alternatives to Silicon nanowires surfaces [9].

3.1. Drop movement and drop microfluidics basic operations

3.1.1. Spinning

Drops can also be spun using a tightly rotating magnetic field on its axis and the commensurate generation of circular motion within the drop may be useful for mixing (see Fig. 4).

3.1.2. Pinning

Drops containing paramagnetic particles can be placed and moved on Si nanowire superhydrophobic surfaces, but in order to place drops that do not contain magnetic particles a surface defect must be present. The surface defect can be created by physical damage or damage to the hydrophobic chemical coating. Physical damage can be created using a sharp point such as a small needle, while the chemical coat can be removed using a laser pulse. In either case, the abrupt change in contact angle in the damaged region pins a water drop that is dropped from above this region. In Fig. 5(a)–(c), the movement of a water drop

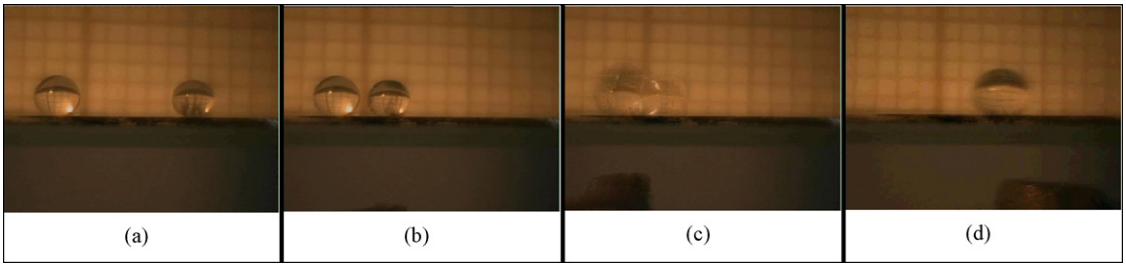

Fig. 5. Sequence of frames showing a pinned water drop (left-most drop in each frame) and a drop moving towards it (a and b), at the moment of coalescence (c) and the resultant drop moving to the right after being depinned (d).

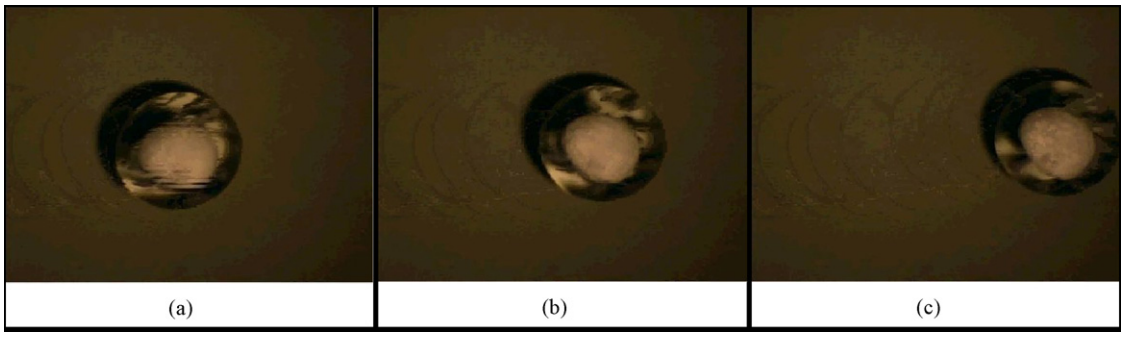

Fig. 6. Sequence of frames from a video showing the movement of a water drop with an expanded polystyrene particle on top (a–c) on a Si NW surface. The drop slides across the surface since the polystyrene particle does not appear to move with respect to the drop as it goes from the left (a) to the right (c) side of the superhydrophobic surface.

containing paramagnetic particles towards a water drop held by pinning and the subsequent coalescence of the drops is shown to illustrate this capability.

3.1.3. Depinning

While drops without paramagnetic particles that are pinned due to a surface defect cannot be moved, when combined with a drop containing paramagnetic particles or when a drop with paramagnetic particles is placed on a surface defect, a magnetic field can be used to force the drop out of the defect. The utility of this action is that two types of drops can be combined and then the combined drop can be moved for further processing. Thus, for example, an aqueous solution to be analyzed can be combined with other drops sequentially for sample pretreatment reasons and subsequently moved to another location for analysis. Depinning takes place with only a very small amount of water left behind on the defect. Visual evidence leads us to believe that the amount of water left on the defect depends on the size of the defect. Such depinning action with essentially all of the liquid being removed from the pinned location has not been previously described in the literature using any type of force. We have indications that this surprising action is performed using the surface tension of the drop as a "lever" and the paramagnetic particles as a "fulcrum" (see Fig. 5(d)).

3.1.4. Coalescence and splitting

Completing the full range of digital microfluidics is the action of splitting a water drop using two magnetic fields [8]. This action can be used in concert with drop combination in order to perform sample pretreatment, dilution, and/or parallel analyses on a single original sample drop. Another reason to split drops is to create smaller drops for analysis. In a recent paper [20], we show that electrodes can be used to measure dopamine and glucose within the drops because drops can be combined and split. Depinning from the electrode can also be accomplished.

3.1.5. Sliding

Another important area of investigation is to determine how drops move across superhydrophobic surface. Mahadevan and Pomeau use scaling arguments to show why nonwetting viscous droplets can roll down an inclined superhydrophobic surface [21]. Richard and Quere [22] explain why for small nonwetting droplets, the smaller the droplet the higher the drop velocity. Both groups distill the basic forces at play when drops move at a constant velocity as the driving force (in their case gravity) versus viscous dissipation. We have done several preliminary experiments to detect whether the drops in our system "slide" or "roll". When a small piece of expanded polystyrene is placed on top of a water drop, it remains virtually motionless as the drop moves across the superhydrophobic nanowire surface. Thus we conclude that the water drop slides along the surface due to the combined effects of a superhydrophobic surface and the very low amount of contact area between the rounded water drop and the nanowire surface (see Fig. 6).

3.1.6. Drop motion model

In order to interpret our results, we determined the basic physics involved in drop motion. When there is no external magnetic field, the particles do not have a permanent magnetic dipole moment and simply sediment to the bottom of the drop. The permanent magnet generates a spatially non-uniform magnetic field on the region were the drop is located. This magnetic field magnetizes the paramagnetic particles that, due to the induced magnetic dipolar interaction, aggregate into clusters that follow the magnetic field lines [23]. When the magnet is displaced, the clusters slide inside the drop following the motion of the magnet until they arrive at the contact line. Fig. 7 shows the force bal-

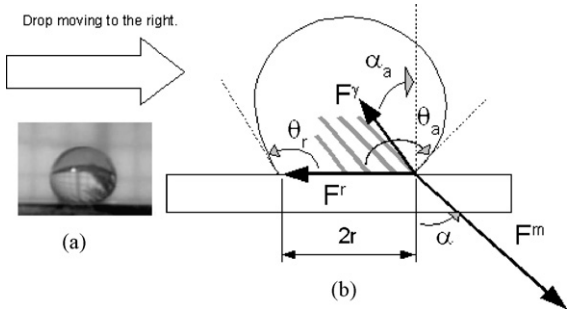

Fig. 7. Forces involved in magnetic drop movement. A picture from a movie (a) shows a water drop moving to the right, with magnetic microparticle clusters climbing along the drop and increasing its advancing angle. The schematic drawing (b) represents a force diagram on the surface of the moving drop; the vertical component of the magnetic force will deform the drop surface at the contact line in the direction of the superhydrophobic surface increasing the contact angle to $\theta_a = \pi - \alpha$.

ance on a drop moving to the right. When the first clusters arrive at the contact line, the competition between the capillary force F^{γ} and the magnetic force F^{m} makes the clusters start to climb along the drop surface (see Fig. 7(b)). Once they reach a specific orientation and position, the clusters pull the drop surface and strongly distort the drop shape. There is clear evidence of dynamically induced contact angle hysteresis, with the advancing contact angle θ_a being larger than the receding contact angle θ_r.

The magnetic force acts along the cluster axis (forming an angle α with the vertical direction) while the capillary force $F^{\gamma} = (\pi\gamma D)/[\cos(\alpha - \alpha_a)]$ acts along the normal axis to the drop surface (forming an angle α_a with the vertical direction). Here D is the diameter of the cluster and γ is the surface tension. The vertical component of the magnetic force will deform the drop surface at the contact line so that the drop surface approaches the superhydrophobic surface, increasing the advancing contact angle θ_a (decreasing $\alpha_a = \pi - \theta_a$). Consequently, the magnetic force generates a difference between the contact angles at the advancing and the receding segments of the contact line. This contact angle difference opposes the drop motion with a retention force that can be expressed as [24] $F^{\gamma} = 2\gamma rJ$, where $r = R\cos(\theta_c - \pi/2)$ is the radius of the circle of contact between the drop and the superhydrophobic surface and $J = \cos\theta_a - \cos\theta_r$. Thus, the total horizontal force balance on the drop can be written as

$$F^{m}\sin\alpha - \frac{\pi\gamma D}{\cos(\alpha - \alpha_a)}\sin\alpha_a - 2\gamma R\cos\left(\theta_c - \frac{\pi}{2}\right) \times(\cos\theta_a - \cos\theta_r) = 0 \quad (1)$$

On the other hand, the vertical force balance reads:

$$F^{m}\cos\alpha - \frac{\pi\gamma D}{\cos(\alpha - \alpha_a)}\cos\alpha_a = 0 \quad (2)$$

If there is no difference between the advancing and receding contact angles, the force balances simply state that the system is in equilibrium provided that $\alpha = \alpha_a$. Instead, when a contact angle difference is generated, the capillary force that opposes contact line motion introduces a threshold that can only be overcome when the inclination of the clusters α, is larger than the advancing contact angle α_a. This is precisely what would happen when the vertical components of magnetic and capillary force compensate, while the magnetic force horizontal component is visibly higher than the corresponding capillary force component. When this excess magnetic force horizontal component is higher than the contact angle difference term, drop motion will occur. From this point of view, large values of α would be more convenient in order to overcome the opposing force due to the contact angle difference.

It may occur that the first cluster arriving at the contact line would not be able to overcome the capillary retention force. Then, the magnet displacement with respect to the drop will keep increasing making the first cluster climb along the drop surface, thus driving more clusters to the contact line. Due to the magnetic field spatial structure, the clusters arriving at the contact line would have a larger inclination and would yield a comparatively stronger contribution to the horizontal component of the magnetic force than to the vertical one. Consequently, the advancing contact angle would be slightly perturbed, while the horizontal force will increase significantly and drop motion will occur. This is precisely what happens in the experiments, as shown in the side view of the moving drop in Fig. 7(a), where the contact angle difference and the inclination of the clusters can be appreciated.

A full numerical check of the above expressions is not possible; however, because precise values concerning the size and the number of the clusters would be needed. This possibility is precluded by the lens effect of the drop surface. Nevertheless, calculations based on the actual measured values of the angular variables of the problem ($\theta_c \approx 147^\circ$, $\theta_a \approx 160^\circ$, $\theta_r \approx 136^\circ$, and $\alpha \approx 44^\circ$) show that the order of magnitude of the magnetic force modulus needed to balance the capillary and retention forces is within the range achievable in our experimental setup.

Another interesting aspect is the role of the magnet velocity in the initiation of the drop motion. Actually, the magnet displacement entrains the cluster structure in its motion. Before the threshold condition for drop motion is achieved, the drop is standing and the clusters move through it with possibly large velocities. In order to make some estimations, the clusters in the experiments can be approximated as circular cylinders with diameter $D = 100$ nm. These clusters may move within the standing drop at speeds up to 10 cm/s, yielding a Reynolds number $Re = \rho VD/\mu \approx 10$. This means that fluid inertial effects may be important at these high magnet speeds.

3.2. Fluid viscosity and drop movement

In order to determine whether operating conditions need to be altered in order to move viscous drops, we conducted a series of experiments using aqueous solutions of Dextran 428. As seen in Table 1, the range of viscosities exceeds the range expected to be found in biological fluids and is sufficiently large to determine what influence viscosity has on drop movement. When paramagnetic particles are added to achieve a consistent concentration of 2 wt% for these solutions of Dextran 428, we observed no difficulty in moving drops with viscosities up to 125 mPa s along a superhydrophobic polyethylene surface. Drops with viscosities up to approximately 460 mPa s can be moved on Si NW surfaces using iron particle concentrations as low as 0.5%. Fig. 8 shows eight frames of digital videos captured for movement of drops at 0, 5, 10 and 20% Dextran. The clusters' lengths and distributions vary from drop to drop. However, it has been observed that in general, for both surfaces and for the viscosity range studied, the clusters at the front of the drop have a higher angle with respect to the bottom of the drop than those clusters at the back of the drop, since the back part is further from the magnet axis (Fig. 8). In each movie, drops are moved several times over the same surface to ensure repeatability, durability of the surface, and consistency in observations. In Fig. 8, video analyses of dextran solution drops designed to investigate the effect of viscosity on drop movement for LPDE surfaces suggest that paramagnetic particle chain orientation compensates for viscosity increases

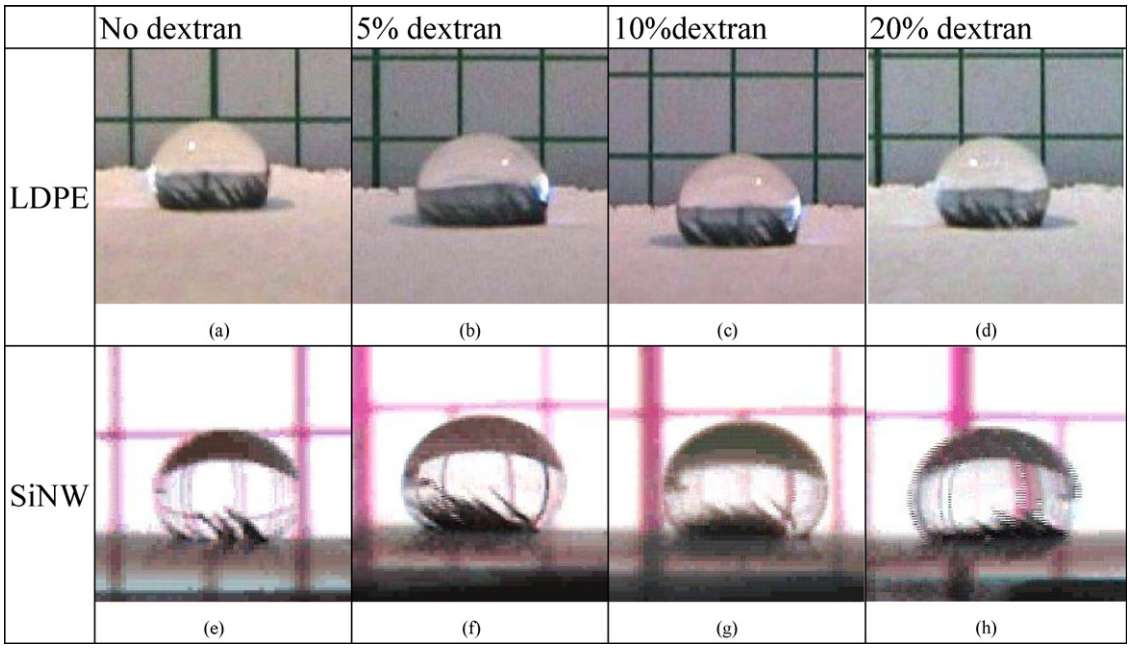

Fig. 8. Still frames from eight different movies of drop movement on LDPE (a–d) and Si NW (e–h) surfaces. Water (a and e) and aqueous drops with 5% (b and f), 10% (c and g) and 20% (d and h) Dextran 428 move to the left using micro-scale fluidics controlled by magnetic fields. The clusters' lengths and distributions varies from drop to drop, but it has been observed that in general, for both surface types and all viscosities, the clusters at the front of the drop have a higher angle with respect to the bottom of the drop than those at the back, since the back of the drop is further from the magnet axis.

from 1.2 mPa s (water drop) to 125 mPa s (20%, w/v—Dextran 428) in order to maintain drop movement. Interestingly, such changes in chain orientation are not present for drops moving on Si NW surfaces even at higher viscosities of 470 mPa s (30% w/v—Dextran 428). At least five drop pictures were taken from each video, and all the observable clusters within each drop were measured and averaged using the angle analysis tool included in the ImageJ software program (NIH, USA). The most notable difference among the movies is a relatively subtle but detectable change in the maximum angle formed between an imaginary line parallel to the bottom of the drop and the superhydrophobic surface, and the line made by the paramagnetic clusters when the drop is in motion ($90^\circ - \alpha$ in Fig. 7). This is most notable in the 20% (w/v) dextran drop using LDPE surfaces where the particles can climb up the drop wall until they are nearly parallel to the plane of the superhydrophobic surface.

Since the magnet is manipulated by hand in these experiments, some fluctuations in the field strength felt by the paramagnetic particles does occur. However, it is evident that the maximum angle formed with respect to a line orthogonal to the surface can achieve higher values at higher viscosities for LDPE surfaces. It is logical that drops with lower resistance to drop movement will not experience as high an angle since the drop would be more easily displaced, and thus the maximum angle is indicative of the amount of force needed in the direction of flow in order to maintain a constant velocity.

For drop movement, typical values of Reynolds, Capillary, and Bond numbers are 10, 1.4×10^{-4}, and 0.14, respectively. These relatively low values indicate that the flow is in the Stokesian regime, the shape of the drop is relatively unchanged during drop movement, and inertial effects are negligible. When the drop is moving at constant velocity, the horizontal component of the magnetic force should balance the capillary, retention, and friction forces. Frictional driving force can be estimated as a generalized Stokesian flow resistance as $F^{\mathrm{h}} = 6\pi\eta V\beta$ with η as the fluid viscosity, V the drop velocity, and β is a geometric factor [25,26]. Thus, for constant drop velocity and magnetic field strength the particle chain angle α with respect to the drop's vertical axis should be proportional to the liquid viscosity. If the viscosity is too high, then drop movement may not be possible for a given paramagnetic particle concentration and hence a higher concentration is needed to overcome frictional resistance.

Fig. 9 shows the trend of α as a function of aqueous solution viscosity measured for different superhydrophobic LDPE surfaces. The graph illustrates the general trend that the angle increases with the viscosity of drops. However the trend does not appear to be linear for high viscosities. Deviations from linearity at high viscosities are thought to be primarily due to the difficulty of controlling the number of chains formed in the drop as well as the inherent heterogeneity of the surfaces. It is also shown that drops with higher viscosity are able to move when adding higher concentration of particles.

For superhydrophobic surfaces with advancing and receding contact angles near 180°, it is difficult to characterize small differences in their contact zone due to subtle morphological differences among substrates (assuming that the surface chemistry is uniform) as well as changes in the contact zone as a function of magnetic particle concentration and field strength. However, by keeping all other variables constant the differences in the slope of chain angle versus viscosity may offer an alternate method of characterizing superhydrophobic surfaces. The steeper the slope of α versus drop viscosity, the more frictional resistance is present for a superhydrophobic surface. Thus using micro-scale drop movement via magnetic control with

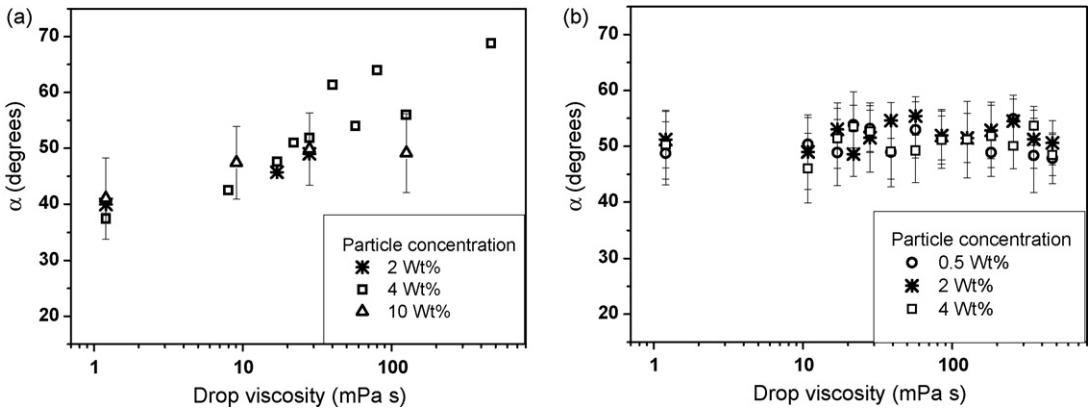

Fig. 9. Plot of the angle α between the clusters axis and the drop's vertical axis as a function of drop viscosity on a LDPE (a) and a Si NW (b) superhydrophobic surfaces. The percentage of iron microparticles is 2, 4 and 10 wt% for the LDPE surface and 0.5, 2 and 4% for the Si NW surface. Data points correspond to the average of the angles of all the observable clusters in at least five drop pictures of the same viscosity and iron microparticle composition; the error bars correspond to the standard deviation. Data points with no error bars correspond to the angle of one representative cluster on a single picture.

drops of different viscosities could prove to be a useful method to identify the better morphologies that reduce resistance to flow.

Although Subramaninan and co-workers [25,26] derive an analytical form of the hydrodynamic resistance for a drop spreading on a flat surface, it is not readily applicable to superhydrophobic surfaces. The contact area of drops on superhydrophobic surfaces depends upon the shape of the liquid in contact with the rough surface. Given the distortion of the drop by the paramagnetic particles and the low-contact area due to the high degree of roughness, it is difficult to ascertain what fraction of the surface will actually be in contact with liquid. Moreover, the geometric parameter will change in our system when paramagnetic particle concentrations are varied as well as when other parameters are changed such as magnetic field strength and surface morphology. Instead, observations of drop motion for different drop viscosities will help experimentally determine the geometric parameter, albeit lumped with the effective magnetic force driving drop motion.

4. Conclusions

Combining the small resistance to drop movement inherent to superhydrophobic surfaces with magnetic control of particles leads to a new micro-scale drop fluidic method. Fluorinated silicon nanowires surfaces and low-density polyethylene microcrystalline surfaces are two examples of superhydrophobic surfaces that can reduce resistance to drop movement to the extent needed for drop movement. Using paramagnetic particles of high-magnetic saturation permits relatively low concentrations such as 0.1 wt% to be sufficient for magnetic control of drops. An interesting compensation for liquid viscosity observed in this method entails aligning the induced magnetic force component along the direction of flow in order to increase the net force in that direction. Results with LDPE superhydrophobic surfaces confirm theoretical predictions that paramagnetic particle cluster angle is proportional to drop viscosity. Silicon nanowire superhydrophobic surfaces show little effect of viscosity on particle cluster angle presumably due to their much lower resistance to drop movement.

References

[1] J. Bico, C. Marzolin, D. Quere, Pearl drops, Europhys. Lett. 47 (1999) 220–226.
[2] A. Lafuma, D. Quere, Superhydrophobic states, Nat. Mater. vol. 2 (2003) 457–460.
[3] T. Onda, S. Shibuichi, N. Satoh, K. Tsujii, Super-water-repellent fractal surfaces, Langmuir 12 (1996) 2125–2127.
[4] R.N. Wenzel, Resistance of solid surfaces to wetting by water, Ind. Eng. Chem. 28 (1936) 988–994.
[5] R.D. Hazlett, Fractal applications: wettability and contact angle, J. Colloid Interf. Sci. (1990).
[6] A.B.D. Cassie, S. Baxter, Wettability of porous surfaces, Trans. Faraday Soc. 40 (1944) 546–551.
[7] N.A. Patankar, On the modeling of hydrophobic contact angles on rough surfaces, Langmuir 19 (2003) 1249–1253.
[8] A. Egatz-Gómez, S. Melle, A.A. García, S.A. Lindsay, M. Márquez, P. Domínguez-García, M.A. Rubio, S.T. Picraux, J.L. Taraci, T. Clement, Discrete magnetic microfluidics, Appl. Phys. Lett. 89 (2006) 034106.
[9] A. Egatz-Gómez, J. Schneider, P. Aella, D. Yang, P. Domínguez-García, S. Lindsay, S.T. Picraux, M.A. Rubio, S. Melle, M. Marquez, Silicon nanowire and polyethylene superhydrophobic surfaces for discrete magnetic microfluidics, Appl. Surf. Sci. 254 (2007) 330–334.
[10] A.A. García, A. Egatz-Gómez, S.A. Lindsay, P. Domínguez-García, S. Melle, M. Marquez, M.A. Rubio, S.T. Picraux, D. Yang, P. Aella, Magnetic movement of biological fluid droplets, J. Magn. Magn. Mater. 311 (2007) 238–243.
[11] M.S. Park, J.W. Chung, Y.K. Kim, S.C. Chung, H.S. Kho, Viscosity and wettability of animal mucin solutions and human saliva, Oral Dis. vol. 13 (2007) 181–186.
[12] S.R. Hodges, O.E. Jensen, J.M. Rallison, Sliding, slipping and rolling: the sedimentation of a viscous drop down a gently inclined plane, J. Fluid Mech. 512 (2004) 95–131.
[13] X. Lu, C. Zhang, Y. Han, Low-density polyethylene superhydrophobic surface by control of its crystallization behavior, Macromol. Rapid Commun. 25 (2004) 1606–1610.
[14] H.Y. Erbil, A.L. Demirel, Y. Avci, O. Mert, Transformation of a simple plastic into a superhydrophobic surface, Science 299 (5611) (2003) 1377–1380.
[15] S. Melle, M. Lask, G.G. Fuller, Pickering emulsions with controllable stability, Langmuir 21 (2005) 2158–2162.

[16] H. Pu, F. Jiang, Z. Yang, Studies on preparation and chemical stability of reduced iron particles encapsulated with polysiloxane nano-films, Mater. Lett. 60 (2006) 94–97.
[17] M. Hoorfar, M.A. Kurz, Zdenka Policova, M.L. Hair, A. Wilhelm Neumann, Do polysaccharides such as dextran and their monomers really increase the surface tension of water? Langmuir 22 (1) (2006) 52–56.
[18] E. Rotureau, E. Dellacherie, A. Durand, Viscosity of aqueous solutions of polysaccharides and hydrophobically modified polysaccharides: application of Fedors equation, Eur. Polym. J. 42 (2006) 1086–1092.
[19] Amersham_Biosciences, Dextran fractions, in http://www5.gelifesciences.com/APTRIX/upp00919.nsf/(FileDownload)?OpenAgent&docid=5BADD9A54B90D00CC1256EB400417D9A&file=18115341AA.pdf, 2001.
[20] S. Lindsay, T. Vázquez, A. Egatz-Gómez, S. Loyprasert, A.A. Garcia, J. Wang, Magnetic digital microfluidics with electrochemical detection, Analyst 132 (2007) 412.
[21] L. Mahadevan, Y. Pomeau, Rolling droplets, Phys. Fluids 11 (1999) 2449.
[22] D. Richard, D. Quere, Viscous drops rolling on a tilted non-wettable solid, Europhys. Lett. 48 (1999) 286–291.
[23] S. Melle, M.A. Rubio, G.G. Fuller, Time scaling regimes in aggregation of magnetic dipolar particles: scattering dichroism results, Phys. Rev. Lett. 87 (2001) 115501.
[24] C.G.L. Furmidge, Studies at phase interfaces. I. The sliding of liquid drops on solid surfaces and a theory for spray retention, J. Colloid Sci. 17 (1962) 309.
[25] R.S. Subramanian, N. Moumen, J.B. McLaughlin, Motion of a drop on a solid surface due to a wettability gradient, Langmuir 21 (2005) 11844–11849.
[26] N. Moumen, R.S. Subramanian, J.B. McLaughlin, Experiments on the motion of drops on a horizontal solid surface due to a wettability gradient, Langmuir 22 (2006) 2682–2690.